THE JOURNAL OF BIOLOGICAL CHEMISTRY
Vol. 278, No. 36, Issue of September 5, pp. 34483–34490, 2003

Printed in U.S.A.

Laminin α3 LG4 Module Induces Matrix Metalloproteinase-1 through Mitogen-activated Protein Kinase Signaling*

Received for publication, May 8, 2003, and in revised form, June 23, 2003
Published, JBC Papers in Press, June 24, 2003, DOI 10.1074/jbc.M304827200

Atsushi Utani‡§¶, Yutaka Momota‡§, Hideharu Endo‡, Yoshitoshi Kasuya‖, Konrad Beck, Nobuharu Suzuki‡‡, Motoyoshi Nomizu‡‡, and Hiroshi Shinkai‡**

*From the ‡Department of Dermatology and the ‖Department of Biochemistry and Molecular Pharmacology, Graduate School of Medicine, Chiba University, Chiba 260-8670, Japan, the **Matrix Biology & Tissue Repair Research Unit, Department of Dental Health and Biological Sciences, University of Wales College of Medicine, Cardiff CF14 4XY, United Kingdom, and the ‡‡Graduate School of Environmental Earth Science, Hokkaido University, Sapporo 060-0810, Japan*

The LG4 module of the laminin α3 chain (α3 LG4), a component of epithelial-specific laminin-5, has cell attachment activity and binds syndecan (Utani, A., Nomizu, M., Matsuura, H., Kato, K., Kobayashi, T., Takeda, U., Aota, S., Nielsen, P. K., and Shinkai, H. (2001) *J. Biol. Chem*. 276, 28779–28788). Here, we show that recombinant α3 LG4 and a 19-mer synthetic peptide (A3G756) within α3 LG4 active for syndecan binding increased the expression of matrix metalloproteinase-1 (MMP-1) in keratinocytes and fibroblasts. This induction was inhibited by heparin and required *de novo* synthesis of proteins. In keratinocytes, A3G756 up-regulated interleukin (IL)-1β and MMP-1 expression and an IL-1 receptor antagonist thoroughly inhibited A3G756-mediated induction of MMP-1. A3G756 also activated p38 mitogen-activated protein kinase (p38 MAPK) and extracellular signal-related kinase (Erk). Studies with specific inhibitors of MAPKs showed that p38 MAPK activation was necessary for both IL-1β and MMP-1 induction, but Erk activation was required only for MMP-1 induction. In fibroblasts, IL-1 receptor antagonist did not block A3G756-mediated induction of MMP-1. These results indicated that induction of MMP-1 by α3 LG4 is mediated through the IL-1β autocrine loop in keratinocytes but the mechanism of the induction in fibroblasts is different. Our study suggests that the laminin α3 LG4 module may play an important role in tissue remodeling by inducing MMP-1 expression during wound healing.

Laminin is a heterotrimeric glycoprotein specific to the basement membrane and has many biological functions, including cell adhesion, migration, cell proliferation, differentiation, angiogenesis, and tumor invasion (for reviews, see Refs. 1 and 2). At least 15 laminin isoforms (laminin-1 to -15) have been identified with 11 genetically distinct chains: 5 α chains, 3 β chains, and 3 γ chains. Three chains assemble into a cross-shaped heterotrimer (αβγ) through coiled-coil interaction at the long arm of the cross (3, 4). Laminin-5 is specific to epithelial cells and a component of the anchoring filament. Laminin-5 forms a complex with the hemidesmosome apparatus by interacting with laminin-6 and -7, collagen VII (5, 6), and fibulin-1 and -2 (7, 8). Laminin-5 consists of the α3, β3, and γ2 chains. The α3 chain contains a large globular module (G module)[1] at the C terminus, which consists of a tandem repeat of five homologous LG modules (LG1–LG5), each module containing about 200 amino acid residues autonomous folding unit (9). The LG subdomains of laminin α chains have been shown to bind heparin, $\alpha_3\beta_1$, $\alpha_6\beta_4$ integrins, α-dystroglycan, and syndecan (Ref. 10; for review, see Ref. 11) and are implicated as active regions for various biological functions.

Syndecans, cell surface heparan sulfate proteoglycans, have been shown to bind the G module of laminin α chains and are involved in laminin-mediated biological functions. We previously demonstrated that keratinocytes and fibroblasts bound LG4 of the α3 G module via syndecans (12). Neurite outgrowth of PC12 cells was induced by α3 LG4 via syndecans (13). We also showed that HT1080 cells bound to the C-terminal G module of the laminin α4 chain through syndecans (14). The interaction of laminin α1 LG4 and syndecan family or heparan sulfate proteoglycans was essential for embryonic basement membrane assembly (15).

Although laminin α3 LG4–5 is processed in the keratinocyte culture medium (16, 17), the unprocessed laminin α3 chain was found in a cell layer of the provisional edge of the cell sheet in cultured keratinocytes. *In vivo*, the unprocessed α3 chain has been identified especially in the newly synthesized epidermal basement membrane in wounds but disappears from the mature basement membrane (Refs. 18 and 19; for review, see Ref. 20).

Matrix metalloproteinase-1 (MMP-1) is expressed in the basal keratinocytes at the leading edge of re-epithelization (Refs. 21 and 22; for review, see Ref. 23). At the wound edge, MMP-1 degrades collagen and promotes cell migration and wound closure. The similar temporal and spatial localization of MMP-1 and unprocessed α3 chain led us to study the relationship between MMP-1 induction and signaling pathways induced by the laminin α3 LG4 module. In the present work, we demonstrated that the laminin α3 LG4 module induced MMP-1 expression by the activation of MAPK via syndecan receptor.

* This work was supported by Grant-in-aid 14570798 for Scientific Research from the Ministry of Education, Science, Culture and Sports of Japan and by a grant from the Dermatological Basic Research Shiseido Fund (to A. U.). The costs of publication of this article were defrayed in part by the payment of page charges. This article must therefore be hereby marked "*advertisement*" in accordance with 18 U.S.C. Section 1734 solely to indicate this fact.

§ Both authors contributed equally to this work.

¶ To whom correspondence should be addressed: Dept. of Dermatology, Graduate School of Medicine, Chiba University, Inohana 1-8-1, Chuo-ku, Chiba 260-8670, Japan. Tel.: 81-43-222-7171 (ext. 5332); Fax: 81-43-226-2128; E-mail: utani@derma01.m.chiba-u.ac.jp.

[1] The abbreviations used are: G module, globular module; MMP-1, matrix metalloproteinase-1; MAPK, mitogen-activated protein kinase; IL-1, interleukin-1; GAPDH, glyceraldehyde-3-phosphate dehydrogenase; RT, reverse transcriptase; Erk, extracellular signal-related kinase; PBS, phosphate-buffered saline; FITC, fluorescein isothiocyanate; nt, nucleotide(s); BSA, bovine serum albumin; ELISA, enzyme-linked immunosorbent assay; DMEM, Dulbecco's modified Eagle's medium; HPLC, high performance liquid chromatography.

EXPERIMENTAL PROCEDURES

Cultured Cells—Human neonatal dermal fibroblasts were obtained from Asahi Techno Glass Co. (Tokyo, Japan). 293T cells were derived from 293 cells as temperature-sensitive subclones (24). These cells were maintained in Dulbecco's modified Eagle's medium (DMEM, Invitrogen, Carlsbad, CA) supplemented with 10% fetal bovine serum (Invitrogen), 100 units/ml penicillin, and 50 units/ml streptomycin. Human primary keratinocytes were purchased from Clonetics (San Diego, CA) and maintained in keratinocyte-SFM supplemented with epidermal growth factor and bovine pituitary extracts (Invitrogen). Keratinocytes and fibroblasts were used at the second through fifth passages in the experiments.

Reagents—Anti-phospho-p44/42 MAPK (Erk) polyclonal antibody, anti-phospho-p38 MAPK polyclonal antibody, and anti-phospho-stress-activated protein kinase/c-Jun N-terminal kinase polyclonal antibody were purchased from Cell Signaling Technology (Beverly, MA). Polyclonal antibody to p38 MAPK was a kind gift from Dr. Sudo (Antibiotics Laboratory, RIKEN, Saitama, Japan) (25). Anti-Erk2 monoclonal antibody was purchased from Upstate Biotechnology, Inc. (Waltham, MA). Anti-human IL-1β monoclonal antibody (AF-201-NA) was obtained from R&D Systems (Minneapolis, MN). Anti-human MMP-1 polyclonal antibody (444209) was from Calbiochem (San Diego, CA). Peroxidase-conjugated anti-rabbit and anti-mouse IgG antibodies and ECL (Amersham Biosciences, Uppsala, Sweden) were used for Western blotting. Human syndecan-4 monoclonal antibody (5G9) and human syndecan-2 antibody (L-18) were obtained from Santa Cruz Biotechnology, Inc. (Santa Cruz, CA). Fluorescein isothiocyanate (FITC)-conjugated anti-mouse IgG antibody and Cy3-conjugated anti-human IgG antibody were purchased from Jackson ImmunoResearch Laboratories (West Grove, PA). FITC-conjugated anti-heparan sulfate antibody (10E4) was obtained from Seikagaku Kogyo (Tokyo, Japan). MAPK inhibitors SB202190 and PD98059 were from Calbiochem and dissolved in dimethyl sulfoxide (Me_2SO). IL-1β was obtained from Roche Diagnostics (Indianapolis, IN). Human IL-1 receptor antagonist (IL-1RA, which traps IL-1β) was purchased from R&D Systems. Heparin was from Seikagaku Kogyo and cycloheximide from Sigma.

Recombinant Proteins—Recombinant α3 LG4 was expressed as a chimera with a human IgG Fc portion at the C terminus and purified as previously described with a minor modification (12). Briefly, recombinant proteins were expressed in 293 T cells by the Ca-P transfection kit (Invitrogen). After 24 h, cells were incubated with Chinese hamster ovary medium (Invitrogen) for another 2 days, followed by purification with protein A-Sepharose (Amersham Biosciences).

Synthesis of A3G756—Peptides were manually synthesized by the Fmoc (*N*-(9-fluorenyl)methoxycarbonyl)-based solid-phase methods with a C-terminal amide as previously described (26). Peptides were purified by reverse phase high performance liquid chromatography (HPLC) using a Mightysil RP-18 column (Kanto Chemical Co., Inc., Tokyo, Japan) with a gradient of water/acetonitrile containing 0.1% trifluoroacetic acid. Purity and identity were confirmed by HPLC and by fast atom bombardment mass spectral analysis at the GC-MS & NMR Laboratory, Graduate School of Agriculture, Hokkaido University (Hokkaido, Japan). The A3G756 peptide (residues 1411–1429, KNSFMALYLSKGRLVFALG) showed syndecan-mediated cell attachment in a heparin dependent manner as strong as the previously identified 12-mer active peptide (residues 1412–1423, NSFMALYLSKGR) (12). Peptide S4 (LVAGAFFKRKLLLMNSSGY) was a scrambled peptide of A3G756, and cell adhesion and inhibition assays demonstrated that S4 had no adhesion activity.

Treatment of Cells—Keratinocytes were seeded at 1.0×10^5 in 12-well plastic dishes. After 24 h, early confluent cells were starved for 24 h in keratinocyte-SFM. Fibroblasts (2.0×10^5) were seeded in 12-well dishes, and were settled for several hours until attaching, followed by 24 h of starvation in DMEM containing 0.1% BSA. Then, recombinant protein, peptides, or cytokine were added in 0.4 ml of fresh medium. Cells were pretreated with 2 μg/ml cycloheximide for 2 h before stimulation. MAPK inhibitors, 30 μg/ml SB202190, 20 μg/ml PD98059, or Me_2SO only were added 1 h before stimulation.

RT-PCR Analysis of MMP-1—Total RNA was prepared from cells after 8-h incubation by RNAeasy kit (Qiagen GmbH, Hilden, Germany). cDNA was synthesized from RNA (2.0 μg) with an oligo(dT) primer in a total volume of 21 μl by SPreamplification System (Invitrogen). cDNA (1 μl for IL-1β or 0.1 μl for MMP-1 and GAPDH) was subjected to PCR for amplification. In preliminary experiments, we determined the optimal number of cycles within the linearity of reactions for each PCR product. The cycle number was 35 cycles for IL-1β and was 25 cycles for MMP-1 and GAPDH. The primers for PCR are as follows: human MMP-1 (830–1465 nt, GenBank™ accession no. X54925), forward (5′-CATCCAAGCCATATATGGACG) and backward (5′-GCAGTTGAACCAGCTATTAGC); human GAPDH (292–885 nt, GenBank™ J04038), forward (5′-CCCATCACCATCTTCCAG) and backward (5′-CCTGCTTCACCACCTTCT); human IL-1β (541–1331 nt, GenBank™ M15330), forward (5′-AGCAACAAGTGGTGTTCTCCATG) and backward (5′-CTAGGCTCTTTTACAGACACTGC). Using these primers, PCR was performed by the Expand High Fidelity PCR System (Roche Diagnostics) at 94 °C for 4 min followed by individual cycles at 94 °C for 30 s, 58 °C for 30 s, and 72 °C for 1 min with an extension step of 7 min at 72 °C at the end of the last cycle. The products were separated on 1.5% agarose gel. The bands were visualized with ethidium bromide staining. The intensity of the products was calculated with NIH Image 1.60, and the values were depicted as the ratio to those of GAPDH.

ELISA—Fibroblasts were treated with reagents in 0.4 ml of DMEM containing 0.1% BSA. The triplicate conditioned media were collected, and MMP-1 was measured by the Human Matrix Metalloproteinase 1 ELISA System (Amersham Bioscience) using precoated 96-well immunoplates. Absorbance was read at 450 nm with microplate reader. The MMP-1 level was calculated by standard curve with an internal control following the protocol from the manufacturer.

Western Blotting—Keratinocytes and fibroblasts were treated as described above. Conditioned media were collected. The media were lyophilized and dissolved in 50 μl of sample buffer (20% glycerol, 2% SDS, 125 mM Tris-HCl, pH 6.8, 2% mercaptoethanol, and 0.15% bromphenol blue), and 20 μl of sample was subjected to Western blotting. Cells were washed with ice-cold PBS twice and were lysed on ice by the addition of 40 μl of lysis buffer (20 mM Tris-HCl, pH 7.5, 60 mM glycerophosphate, 10 mM EGTA, 10 mM $MgCl_2$, 10 mM NaF, 2 mM dithiothreitol, 1 mM $N\alpha_3VO_4$, 1 mM phenylmethylsulfonyl fluoride, 5 μg/ml leupeptin, and 1% Nonidet P-40) for 15 min. Cell lysates were cleared by centrifugation at $20,000 \times g$ at 4 °C for 15 min. Aliquot (15 μl) was boiled in sample buffer for 5 min and subjected to 12% SDS-PAGE, and transferred by electroblotting onto polyvinylidene difluoride transfer membranes (Immobilon™, Millipore, Bedford, MA). The membranes were blocked with 10% nonfat milk in Tris-buffered saline (150 mM NaCl, 40 mM Tris-HCl, pH 7.4) plus 0.1% Tween 20, probed with the first antibodies (1:200), and visualized by the peroxidase-conjugated second antibodies (1:2000–1:5000) and an ECL system (Amersham Biosciences). Densitometric analysis was carried out using NIH Image software version 1.60. To verify the amounts of the samples, membrane was probed with anti-p38 MAPK or anti-Erk2 antibody after stripping.

Syndecan-2 and -4 Overexpression in Mammalian Cells—cDNA of whole human syndecan-2 (577–1,245 nt, GenBank™ J04621) and cDNA of whole human syndecan-4 (9–623 nt, GenBank™ X67016) were amplified using mRNA derived from dermal fibroblasts as described previously (12). Briefly, PCR product was subcloned into the expression vector (27) containing a cytomegalovirus promoter and an internal ribosome entry site and puromycine-resistant gene (28). Human primary dermal fibroblasts were transfected by LipofectAMINE (Invitrogen), and clones producing syndecan-2 and -4 were selected with 0.4 μg/ml puromycin (Sigma). Both Western blotting and immunostaining with anti-syndecan-4 antibody confirmed selected syndecan-4-producing clones. The selected syndecan-2-expressing clones were analyzed by Western blotting with anti-syndecan-2 antibody and immunostaining with FITC-anti-heparan sulfate antibody.

Immunocytochemistry—Fibroblasts on cover glass that overexpressed syndecan-2 and -4 were fixed by 4% paraformaldehyde/PBS for 15 min at room temperature and blocked with 5% normal donkey serum (Chemicon International, Inc., Temecula, CA), 1% BSA (Sigma), 0.05% Nonidet P-40 (Sigma), PBS for 15 min. Cells were incubated with recombinant α3 LG4 (10 μg/ml) and anti-syndecan-4 monoclonal antibody (1:50) at 4 °C overnight, followed by Cy3-conjugated anti-human IgG antibody (1:200) and FITC-conjugated anti-mouse IgG antibody (1:200) for 30 min at 37 °C. For syndecan-2 staining, FITC-conjugated anti-heparan sulfate antibody was used. After washing, pictures were taken by Nikon fluorescent microscopy.

Molecular Modeling—A model of the α3 LG4–5 structure was generated using ProMod II version 3.5 (29) with the x-ray derived coordinates of the mouse α2 LG4–5 module pair (Protein Data Bank code 1dyk) (30) as a template, resulting in a final total energy of −3980 kJ/mol. As expected from sequence alignments, the model shows disulfide bonds between Cys-1354 and Cys-1617, Cys-1507 and Cys-1530, and Cys-1682 and Cys-1710.

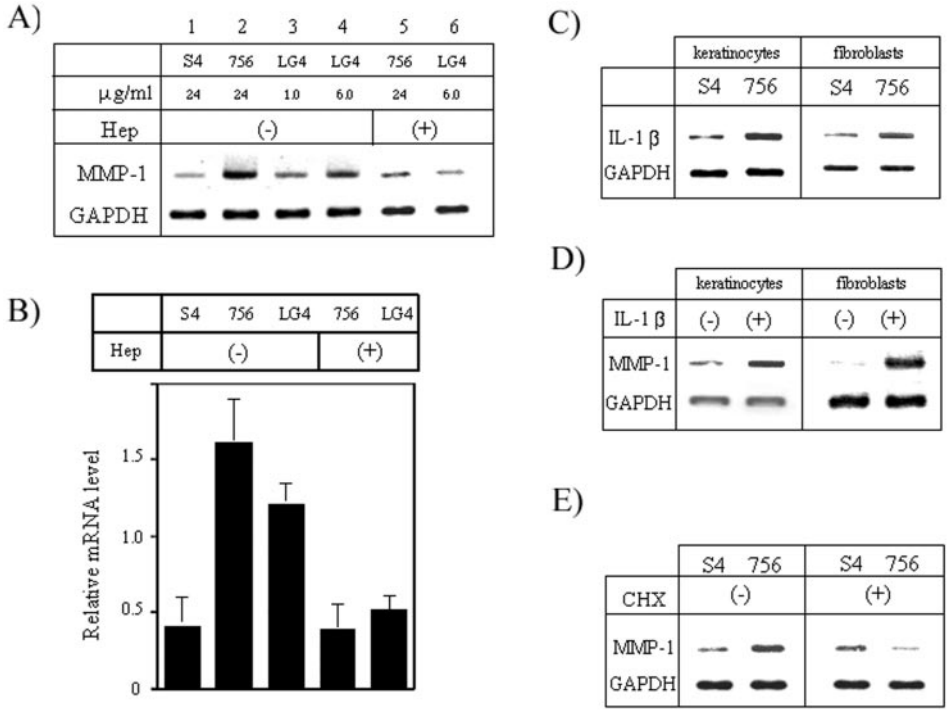

FIG. 1. **MMP-1 gene expression induced by recombinant α3 LG4 and synthetic peptide A3G756.** Recombinant α3 LG4, A3G756, or IL-1β was incubated with keratinocytes and fibroblasts. RNA was prepared at 8-h incubation. Semi-quantitative RT-PCR products were separated on a 1.5% agarose gel and visualized by ethidium bromide staining. *A*, RT-PCR of MMP-1 in keratinocytes. *Lane 1*, control scrambled peptide S4; *lane 2*, A3G756; *lanes 3* and *4*, recombinant α3 LG4; *lane 5*, A3G756 with heparin (30 μg/ml); *lane 6*, recombinant α3 LG4 with heparin (30 μg/ml). *B*, pooled results of RT-PCR analysis. The scanned results were calculated by NIH Image 1.60 and relative mRNA values are shown as the ratio of MMP-1 intensity to that of GAPDH. Data presented are mean ± S.D. of three independent experiments. *C*, RT-PCR of IL-1β was performed using keratinocytes or fibroblasts incubated with 24 μg/ml A3G756 or S4. *D*, the effect of IL-1β (10 units/ml) on MMP-1 gene expression in keratinocytes and fibroblasts. *E*, keratinocytes were incubated with 24 μg/ml A3G756 or S4 in the presence or absence of 2.0 μg/ml cycloheximide (*CHX*). Representative data are shown in three independent RT-PCR experiments in *C–E*.

RESULTS

Laminin α3 LG4 and A3G756 Induce MMP-1 Expression—We previously showed that laminin α3 LG4 and peptide A3G756 within α3 LG4 bind keratinocytes and fibroblasts through syndecans (12). We hypothesized that this interaction regulates expression of MMP-1 during wound healing. Therefore, we examined expression levels of MMP-1 in keratinocyte and fibroblasts when these cells were incubated with α3 LG4 and A3G756. RT-PCR analysis demonstrated that recombinant α3 LG4 and peptide A3G756 stimulated MMP-1 mRNA expression in keratinocytes, whereas control peptide S4 (scrambled A3G756 peptide sequence) did not change MMP-1 mRNA (Fig. 1, *A* and *B*). This increase was strongly blocked by the addition of heparin into the medium (Fig. 1, *A* and *B*). The heparin-dependent MMP-1 induction and syndecan binding to the A3G756 peptide suggest that the induction process is mediated through syndecans.

Because IL-1β is known to induce MMP-1 expression (31, 32), we next examined whether A3G756 increases IL-1β mRNA levels. In both keratinocytes and fibroblasts, A3G756 significantly increased IL-1β mRNA expression (Fig. 1*C*). We also confirmed that IL-1β induced MMP-1 expression in these cell types, agreeing with previous reports (Fig. 1*D*). Because a 4-h incubation with A3G756 was not sufficient to induce MMP-1 gene expression (data not shown), *de novo* synthesis of some factors might be necessary in this induction process. Pretreatment of keratinocytes with cycloheximide, an inhibitor of translation, totally diminished the up-regulation of MMP-1 gene expression by A3G756 (Fig. 1*E*). These results indicate that *de novo* protein synthesis is required for A3G756-mediated MMP-1 induction. On the contrary, cycloheximide did not inhibit up-regulation of IL-1β gene expression (data not shown), suggesting that the up-regulation of IL-1β by A3G756 did not require new synthesis of a factor(s). Thus, IL-1β is a likely candidate responsible for the synthesis of a new factor involved in the up-regulation of MMP-1 by A3G756.

IL-1 Receptor Antagonist Blocks MMP-1 Induction by A3G756 in Keratinocytes but Not in Fibroblasts—To further investigate the mechanism of IL-1β action, we next examined the effect of IL-1 receptor antagonist on A3G756-mediated MMP-1 induction. In keratinocytes, IL-1RA (IL-1 receptor antagonist) at 0.3 μg/ml inhibited the increase of MMP-1 gene expression by A3G756 (Fig. 2*A*). On the contrary, in fibroblasts A3G756 could up-regulate MMP-1 expression in the presence of an even higher concentration of IL-1RA (1.0 μg/ml) (Fig. 2*B*), which is the concentration used by other groups for blocking the IL-1 autocrine loop in dermal fibroblasts (33, 34). Taken together, the results show that the IL-1β autocrine loop is an essential pathway for A3G756-mediated induction of MMP-1 in keratinocytes, but it is not necessary in fibroblasts, even though A3G756 was able to induce IL-1β gene expression (Fig. 1*D*) and exogenously added IL-1β increased MMP-1 gene expression (Fig. 1*C*).

Increase of MMP-1 Protein Levels by A3G756—Increase of the MMP-1 protein by A3G756 in the keratinocytes was demonstrated by Western blotting of the conditioned medium. MMP-1 protein levels increased in the 12–33-h incubations, but not in the 6- and 8-h incubation, whereas protein levels of IL-1β increased within the 6–12-h incubation (Fig. 3*A*). Although IL-1β showed rather rapid disappearance from the conditioned medium, the observation that IL-1β expression preceded the MMP-1 expression were consistent with the facts that newly synthesized IL-1β induced MMP-1 expression in the keratinocytes. The increase of basal expression of MMP-1 at 33-h incu-

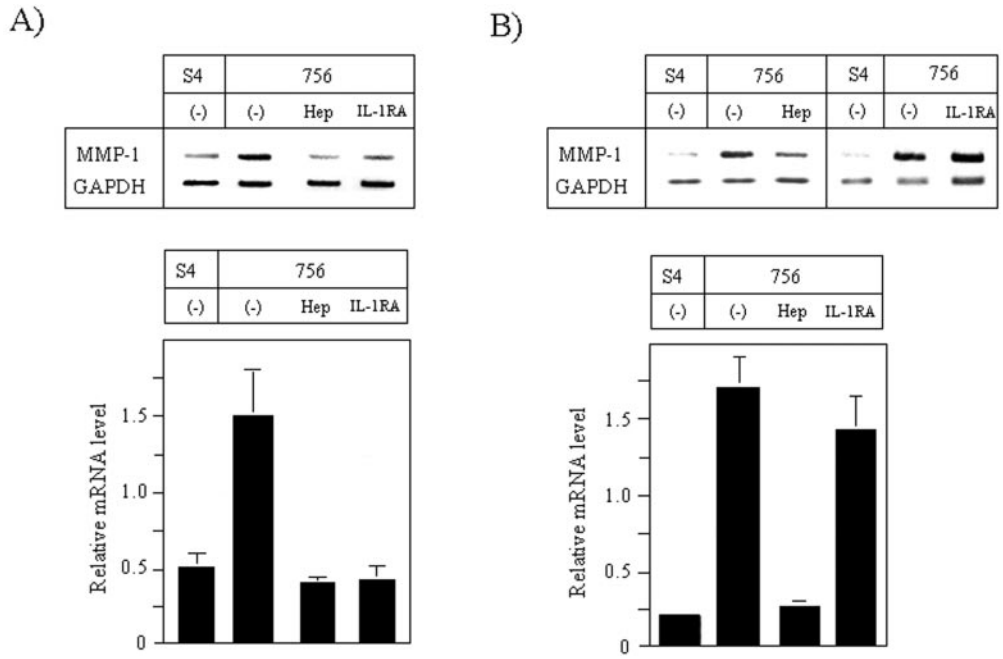

FIG. 2. **IL-1 receptor antagonist inhibits A3G756-mediated MMP-1 induction in keratinocytes but not in fibroblasts.** Keratinocytes (*A*) or fibroblasts (*B*) were incubated for 8 h with S4 or A3G756 peptide (24 μg/ml) with or without heparin (*Hep*) (30 μg/ml) or IL-1 receptor antagonist (*IL-1RA*) (0.3 μg/ml for keratinocytes and 1.0 μg/ml for fibroblasts). *Upper*, RT-PCR products were analyzed on an agarose gel and visualized by ethidium bromide staining. *Lower*, pooled results of RT-PCR. The scanned results of the gels were calculated by NIH Image 1.60, and relative mRNA values are shown as the ratio of MMP-1 intensity to that of GAPDH. Data presented are mean ± S.D. of four independent experiments.

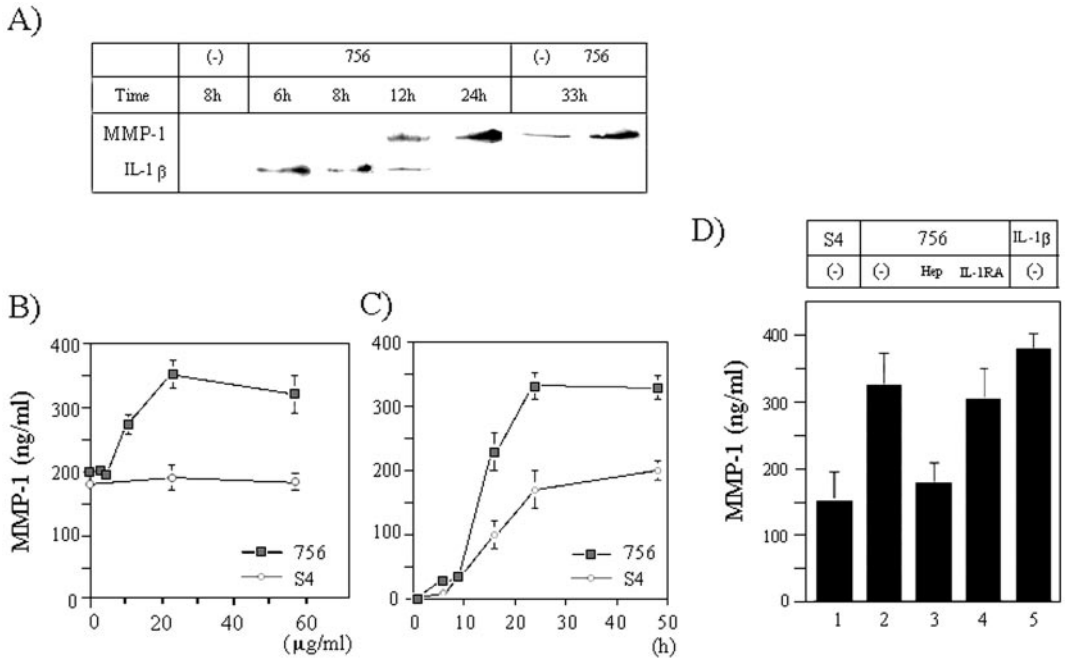

FIG. 3. **A3G756 increases MMP-1 in the conditioned medium of keratinocytes (*A*) and fibroblasts (*B–D*).** *A*, Western blotting analysis of MMP-1 and IL-1β in keratinocyte conditioned medium. Keratinocytes were incubated with 24 μg/ml A3G756 for 6, 8, 12, 24, and 33 h. Conditioned media were collected and lyophilized. The samples were analyzed by Western blotting. Anti-MMP-1 antibody detects a 55-kDa species. Anti-IL-1β antibody reveals a 31-kDa species when the same membrane was used after stripping. Similar expression patterns were observed in two independent experiments. *B*, dose-dependent MMP-1 induction. Fibroblasts were incubated with various amounts of peptides for 24 h. *C*, time course of MMP-1 induction. Fibroblasts were incubated with 24 μg/ml peptides for indicated periods. *D*, fibroblasts were treated with peptides (24 μg/ml) or IL-1β (10 units/ml) for 24 h with or without heparin (30 μg/ml) or IL-1RA (1.0 μg/ml). MMP-1 in the conditioned medium was measured by ELISA. Data presented are mean ± S.D. and are representative results of three independent experiments.

bation without peptide stimulation likely represents the accumulation of MMP-1 protein as also seen in the fibroblasts (Fig. 3*C*). These data confirm that up-regulation of MMP-1 mRNA levels by A3G756 results in increased protein levels. MMP-1 protein levels in fibroblasts were also examined by ELISA using the conditioned medium. A dose-dependent increase in MMP-1 protein levels was observed by incubation of fibroblasts with various amounts of A3G756 in a 24-h incubation (Fig. 3*B*). The MMP-1 protein level reached plateau at 24 μg/ml A3G756. Within the 8-h incubation, protein levels of MMP-1 did not

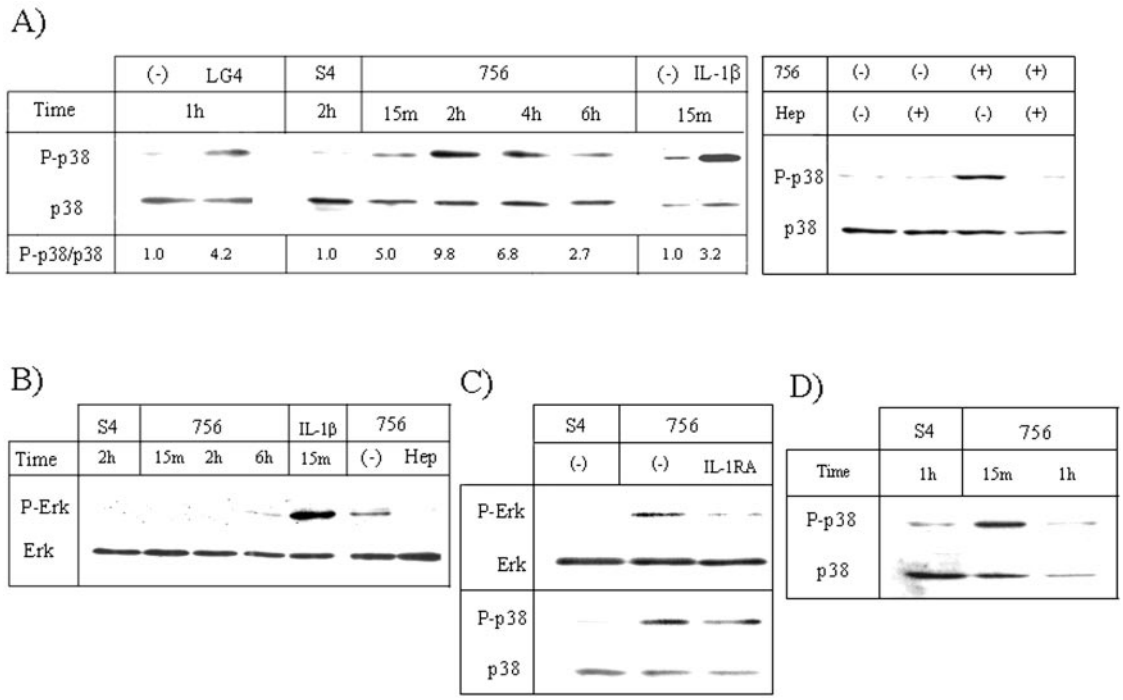

FIG. 4. **MAPK activation by A3G756 in keratinocytes (*A–C*) and fibroblasts (*D*).** Keratinocytes were treated with α3 LG4 (15 μg/ml), S4 (24 μg/ml), A3G756 (24 μg/ml), or IL-1β (10 units/ml) for 15 min to 6 h. Cell lysates were prepared and analyzed by Western blotting. *A*, a membrane was first probed with anti-phosphorylated p38 antibody (*P-p38*) and then successively with anti-p38 antibody after stripping (*p38*). The ratio of the intensity of phosphorylated p38 to that of p38 (*P-p38*/*p38*) was determined using NIH image 1.60, and the ratio of the sample with no stimulation or with control peptide S4 was taken as 1.0. Representative results are shown for three independent experiments. The p38 phosphorylation at 2-h incubation was blocked by the addition of heparin (100 μg/ml) into the medium during incubation. The cells were preincubated with heparin for 15 min before peptide stimulation. Keratinocytes were also examined by Western blotting with anti-phosphorylated Erk (*P-Erk*) and then successively with anti-Erk antibody after stripping (*Erk*). A3G756 activated Erk at 6-h incubation, and this activation was blocked by the addition of heparin. *C*, keratinocytes were incubated with A3G756 or S4 for 6 h in the presence or absence of IL-1RA (0.3 μg/ml), and cell lysates were subjected to Western blotting. *D*, fibroblasts were incubated with S4 or A3G756 for 15 min and 1 h. Similar results were obtained in three independent experiments in *B–D*.

change significantly, but after 16 h of incubation, it increased and the reached its maximum level by 24 h (Fig. 3*C*). AG756-mediated induction of MMP-1 protein was inhibited by heparin but not by IL-1 receptor antagonist in fibroblasts (Fig. 3*D*). Exogenous IL-1β induced MMP-1 expression in fibroblasts (Fig. 3*D*), and IL-1 receptor antagonist blocked the IL-1β-mediated induction (data not shown). The failure of the IL-1 receptor antagonist to inhibit A3G756-mediated MMP-1 induction in fibroblasts suggests that IL-1β is not necessary for MMP-1 induction, although exogenous IL-1β induced MMP-1 expression. These results were consistent with those of mRNA changes in fibroblasts.

A3G756 Activates MAPK Signaling—Because IL-1β is known to activate MAPKs, activation of MAPKs was analyzed by Western blotting with anti-phosphorylated MAPK antibodies (Fig. 4). Treatment of keratinocytes with recombinant α3 LG4 or A3G756 activated p38 MAPK (Fig. 4*A*). Activation of p38 MAPK by A3G756 was observed after 15 min of incubation and reached the maximum level at 2 h. A3G756 also activated Erk within 6 h of incubation (Fig. 4*B*). During these incubation periods, c-Jun N-terminal kinase was not activated (data not shown). As expected, exogenous IL-1β activated both p38 MAPK and Erk in keratinocytes at 15-min incubation (Fig. 4A, 4*B*). Activations of p38 MAPK and Erk by A3G756 were completely blocked by the addition of heparin (Fig. 4, *A* and *B*). These results indicate that A3G756 induces rapid activation of p38 MAPK and slow activation of Erk in keratinocytes. The activation of Erk was drastically inhibited by the addition of IL-1 receptor antagonist, but p38 MAPK activation was partially blocked (Fig. 4*C*). These findings suggest that the Erk activation observed at 6-h incubation was predominantly mediated by the IL-1β autocrine loop. Although at least a part of p38 MAPK activation at 6-h incubation with A3G756 was mediated by the IL-1β autocrine loop, there should be another pathway, *e.g.* a direct activation of p38 MAPK.

In fibroblasts, p38 MAPK was phosphorylated at 15-min incubation and returned to a basal level after 1-h incubation with A3G756 (Fig. 4*D*). Erk activation was not detectable from 15 min to 6 h of incubation, and p38 MAPK was not activated from 2 to 6 h of incubation (data not shown). These different profiles of MAPK activation indicate that A3G756-syndecan binding transduces signals in a cell type-specific manner.

The Effects of MAPK Inhibitors on A3G756 Induction of MMP-1 or IL-1β—Because A3G756 activated p38 MAPK and/or Erk, we examined whether MAPK inhibitors block the up-regulation of MMP-1 by A3G756. RT-PCR analysis showed that SB202190, a specific inhibitor of p38 MAPK, blocked the up-regulation of MMP-1 and IL-1β in keratinocytes (Fig. 5*A*). PD98059, an inhibitor of Erk, blocked the up-regulation of MMP-1, but did not change the IL-1β induction (Fig. 5*A*). Together with the observation that Erk activation was inhibited by IL-1 receptor antagonist, these results indicate that Erk is involved in the up-regulation of MMP-1 through the IL-1β autocrine loop in keratinocytes.

In fibroblasts, PD98059 inhibited both MMP-1 and IL-1β mRNA induction, whereas SB202190 inhibited only IL-1β mRNA induction (Fig. 5*B*). There are two differences in the responses to MAPK inhibitors. One is that both p38 MAPK and Erk activation are required for IL-1β mRNA induction. The other is that blockade of IL-1β mRNA induction by SB202190 did not abolish the MMP-1 induction. These results suggest that IL-1β is not involved in A3G756-mediated MMP-1 induc-

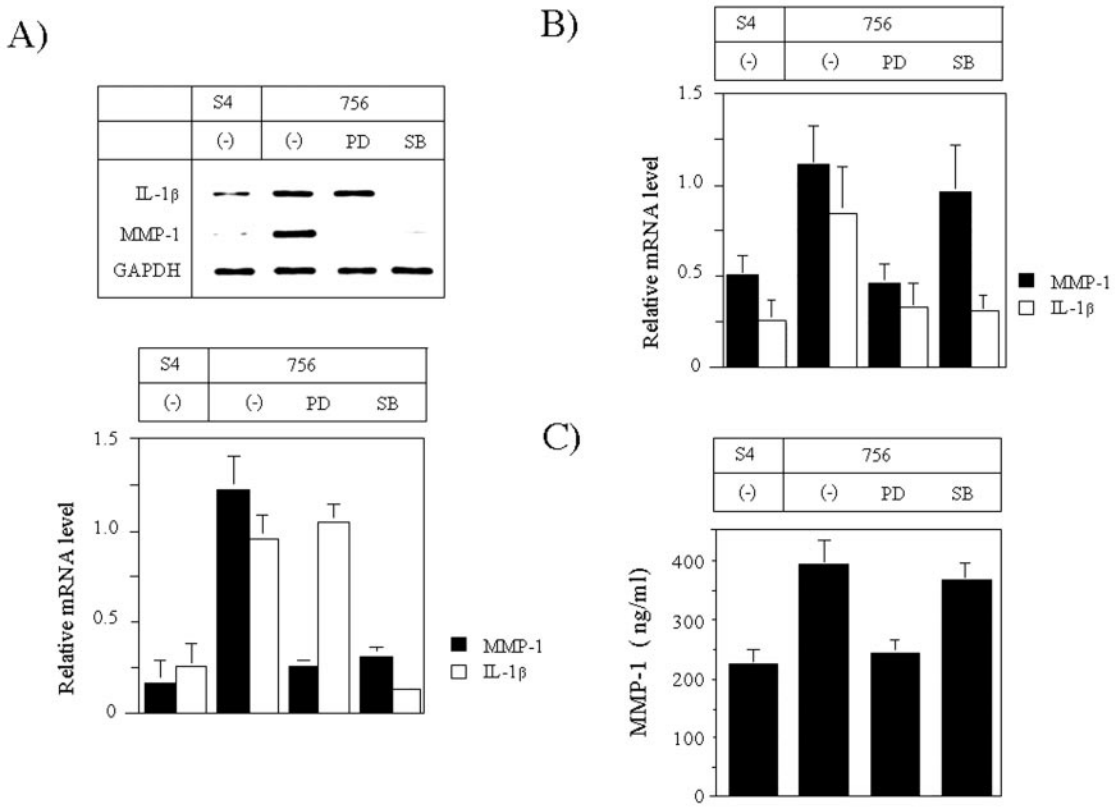

FIG. 5. **The effects of MAPK inhibitors on A3G756-mediated MMP-1 or IL-1β induction.** Keratinocytes (*A*) or fibroblasts (*B* and *C*) were incubated with 24 μg/ml S4 or A3G756 in the presence of PD98059 (20 μg/ml) (*PD*) or SB202190 (30 μg/ml) (*SB*) for 8 h, and then RNA was prepared. *A*, electrophoresis of RT-PCR products and pooled data of RT-PCR are shown. Scanned results were calculated by NIH Image 1.60. The relative values are shown as the ratio of the intensity of MMP-1 or IL-1β to that of GAPDH. Data presented are mean ± S.D. of five independent experiments in *A* and *B*. *B*, pooled data of RT-PCR in fibroblasts. *C*, the fibroblast culture medium was collected after 24-h incubation with peptides in the presence or absence of PD98059 or SB202190 and analyzed by ELISA. Data are mean ± S.D. of three independent experiments.

tion in fibroblasts. Similar patterns were obtained in MMP-1 protein levels estimated by ELISA in fibroblasts (Fig 5*C*). PD98059, but not SB202190, completely blocked the increase of MMP-1 protein levels by A3G756. Only Erk activation is necessary for A3G756-mediated MMP-1, although Erk activation could not be demonstrated in fibroblasts by Western blotting as mentioned (Fig. 4*D*).

Colocalization of α3 LG4 and Syndecans—Previously we showed that α3 LG4 and A3G756 bind keratinocytes and fibroblasts through syndecans in solid phase binding assays (12). Here we demonstrate that soluble α3 LG4 is colocalized with syndecans on the cell surface of dermal fibroblasts (Fig. 6). For this experiment, we obtained dermal fibroblast cell lines that were stably transfected with the expression vector for syndecan-2 or syndecan-4. Incubation of syndecan-expressing fibroblasts with α3 LG4 showed colocalization of α3 LG4 with syndecan-2 or syndecan-4 in double immunostaining (Fig. 6). The α3 LG4 binding was completely diminished by the addition of heparin (30 μg/ml) in both clones during the incubation (data not shown). These results confirm that α3 LG4 interacts with syndecans on the cell surface.

DISCUSSION

In this report, we found that the α3 LG4 module of laminin-5 induces MMP-1 expression by activating the MAPK signaling pathway. We also found that this process involves the IL-1β autocrine loop in keratinocytes. The α3 LG4-mediated induction of MMP-1 occurs through the interaction of syndecans with the A3G756 sequence within the module. Therefore, we are interested in the structure of the α3 LG4 module and the location of the active A3G756 site within the module structure. Although the structure of the LG4–5 module of laminin α3 is not known, the crystal structure of the LG4–5 domain pair of laminin α2 was reported (30). Fig. 7 shows the structure-sequence-based alignment of human α3 LG4–5 generated using the murine α2 LG4–5 structure as a template. The basic residues, Lys (Lys-1421) and Arg (Arg-1423), critical for syndecan binding (12) are exposed and clustered within the sequence of A3G756 (residues 1411–1429; KNSFMALYLSKGRLVFALG) within the LG4 module, which consists of 14 β strands forming a β-sheet sandwich. These two residues are located at one end of a cleft formed by the loop connecting β strands. This cleft contains several further surface-exposed basic residues that might provide a specific orientation to the extended glycosaminoglycan chains by interaction with their sulfate groups. This would be consistent with the active bases of α2 LG4–5 for α-dystroglycan and heparin binding. These results suggest that the A3G756 site of laminin α3 is exposed on the surface of the α3 LG4 structure and is active for syndecan binding.

It has been reported that exogenous IL-1β activates p38 MAPK and leads to up-regulation of MMP-1 expression in fibroblasts (31, 32). Inhibitor of p38 MAPK blocked A3G756-mediated IL-1β expression in keratinocytes (Fig. 5). However, IL-1 receptor antagonist could not completely inhibit p38 MAPK activation in keratinocytes (Fig. 4*C*). Therefore, p38 MAPK is likely involved in both pathways, one from syndecan to IL-1β up-regulation and the other from IL-1β receptor to MMP-1 up-regulation. Erk activation was detected as early as 6 h after incubation with keratinocytes. The activation of Erk was drastically inhibited by the addition of IL-1 receptor antagonist. Further, PD98059, an inhibitor of Erk, did not block

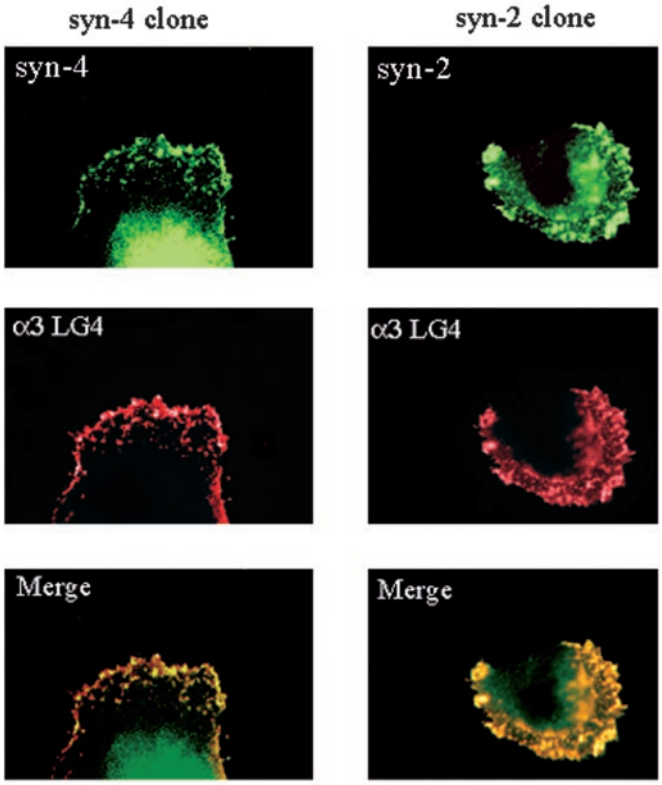

FIG. 6. **Colocalization of α3 LG4 with syndecans in fibroblasts.** Overlay analysis of immunostaining of recombinant α3 LG4 and syndecan-4 (*left column*) or syndecan-2 (*right column*) in fibroblasts. Dermal fibroblasts overexpressing syndecan were fixed on a cover glass and incubated with 10 μg/ml recombinant α3 LG4 in solution. The bound α3 LG4 were visualized with Cy3-conjugated anti-human IgG antibody. Syndecan-4 was detected by anti-syndecan-4 monoclonal antibody (*syn-4*), and syndecan-2 was recognized by FITC-conjugated anti-heparan sulfate monoclonal antibody (*syn-2*). The *bottom panels* are merged images of the *top two pictures* of each *column*. Original magnification, ×400.

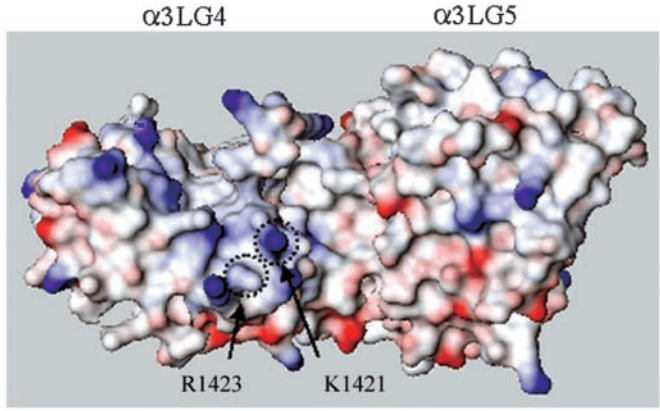

FIG. 7. **Structure of laminin α3 LG4–5 module pair.** A model of the structure of the α3 LG4–5 module pair was generated with ProMod II using the mouse α2 LG4–5 x-ray coordinates (Protein Data Bank code 1dyk) as a template (30). The electrostatic surface potential is shown using a probe radius of 1.4 Å. Negative and positive potential is depicted by *red* and *blue coloring*, respectively. The surface-exposed charged groups of Lys-1421 and Arg-1423 are highlighted, as these residues have been found to be involved in syndecan binding (12). Further positive charges along the cleft might interact with sulfate groups of glycosaminoglycan chains.

A3G756-mediated IL-1β induction in keratinocytes. Therefore, it is likely that Erk mediates signaling from IL-1β receptor to MMP-1 gene expression. Because Erk activation by exogenous IL-1β in keratinocytes is mediated by epidermal growth factor receptor transactivation (35), Erk activation via the syndecan-IL-1β pathway may be induced by a similar mechanism.

We showed that exogenous IL-1β stimulated MMP-1 gene expression and that A3G756 up-regulated IL-1β gene expression in fibroblasts (Fig. 1). Therefore, the involvement of the IL-1β autocrine loop in A3G756-mediated induction of MMP-1 in fibroblasts is possible. However, in fibroblasts, IL-1β autocrine loop and MMP-1 up-regulation likely occur by an independent mechanism. Unlike keratinocytes, p38 MAPK activation was not needed for A3G756-mediated induction of MMP-1 in fibroblasts (Fig. 5*B*). It was reported that, in fibroblasts, basic fibroblast growth factor-mediated induction of MMP-1 required activation of Erk, but not p38 MAPK (32). Signaling from syndecan may up-regulate and/or activate another factor(s) for MMP-1 up-regulation through Erk, independent of the IL-1β autocrine pathway in fibroblasts.

There are four mammalian syndecans, all of which are transmembrane heparan sulfate proteoglycans. Syndecans bind to extracellular matrices as a cell surface receptor and store fibroblast growth factors and vascular endothelial growth factors (for review, see Refs. 36 and 37). Syndecan-1 is the major syndecan of epithelial cells, syndecan-2 is that of mesenchymal cells, and syndecan-3 is that of neural tissues. Syndecan-4 is widely distributed. Usually, more than one syndecan are expressed in a single cell type. The carboxyl terminus of a short cytoplasmic module is conserved in the syndecan family and can interact with syndecan type-specific PDZ-domain-containing proteins. With these signal-transducing molecules, syndecans may have unique functions other than cell adhesion. It is conceivable that a different set of syndecan isoforms expressed at the cell surface of keratinocytes (syndecan-1 and -4) and fibroblasts (syndecan-2 and -4) may play a key role in regulating different responses to laminin α3 LG4. Activating antibody to $\alpha_5\beta_1$ integrin increases MMP-1 gene expression via the IL-1α autocrine loop in fibroblasts (38). Recently, it was reported that the signal from syndecan-4, but not from syndecan-2, transactivates integrin β_1 (39). Taken all together, these results suggest that signals from syndecan binding to laminin α3 LG4 may activate integrins, resulting in MMP-1 induction.

Keratinocytes are known to produce MMPs when they contact collagen fibers at a wound site. MMP-1 degrades collagen I, allowing keratinocytes to migrate on the wound granulation tissue under desiccated eschar. It is also possible that syndecan binding to laminin α3 LG4 contributes to re-epithelization with two different activities such as cell adhesion and MMP-1 induction. The identification of the precise mechanisms of how syndecan binding to laminin α3 LG4 can induce MMP-1 gene expression may lead to the development of clinical applications for wound healing.

Acknowledgment—We appreciate Dr. Yoshihiko Yamada (NIDCR, National Institutes of Health, Bethesda, MD) for critically reading this manuscript.

REFERENCES

1. Timpl, R. (1996) *Curr. Opin. Cell Biol.* **8,** 618–624
2. Colognato, H., and Yurchenco, P. D. (2000) *Dev. Dyn.* **218,** 213–234
3. Utani, A., Nomizu, M., Timpl, R., Roller, P. P., and Yamada, Y. (1994) *J. Biol. Chem.* **269,** 19167–19175
4. Utani, A., Nomizu, M., Sugiyama, S., Miyamoto, S., Roller P. P., and Yamada, Y. (1995) *J. Biol. Chem.* **270,** 3292–3298
5. Rousselle, P., Keene, D. R., Ruggiero, F., Champliaud, M. F., Rest, M., Burgeson, R. E. (1997) *J. Cell Biol.* **138,** 719–728
6. Chen, M., Marinkovich, M. P., Veis, A., Cai, X., Rao, C. N., O., Toole, E. A., and Woodley, D. T. (1997) *J. Biol. Chem.* **272,** 14516–14522
7. Sasaki, T., Gohring, W., Mann, K., Brakebusch, C., Yamada, Y., Fassler, R., and Timpl, R. (2001) *J. Mol. Biol.* **314,** 751–763
8. Utani, A., Nomizu, M., and Yamada, Y. (1997) *J. Biol. Chem.* **272,** 2814–2820
9. Talts, J. F., Mann, K., Yamada, Y., and Timpl, R. (1998) *FEBS Lett.* **426,** 71–76
10. Hoffman, M. P., Nomizu, M., Roque, E., Lee, S., Jung, D. W., Yamada, Y., and Kleinman, H. K. (1998) *J. Biol. Chem.* **273,** 28633–28641
11. Timpl, R, Tisi, D., Talts, J. F., Andac, Z., Sasaki, T., and Hohenester, E. (2000) *Matrix Biol.* **19,** 309–317

12. Utani, A., Nomizu, M., Matsuura, H., Kato, K., Kobayashi, T., Takeda, U., Aota, S., Nielsen, P. K., and Shinkai, H. (2001) *J. Biol. Chem.* **276,** 28779–28788
13. Kato, K., Utani, A., Suzuki, N., Mochizuki, M., Yamada, M., Nishi, N., Matsuura, H., Shinkai, H., and Nomizu, M. (2002) *Biochemistry* **41,** 10747–10753
14. Okazaki, I., Suzuki, N., Nishi, N., Utani, A., Matsuura, H., Shinkai, H., Yamashita, H., Kitagawa, Y., and Nomizu, M. (2002) *J. Biol. Chem.* **277,** 37070–37078
15. Li, S., Harrison, D., Carbonetto, S., Fassler, R., Smyth, N., Edgar, D., and Yurchenco, P. D. (2002) *J. Cell Biol.* **157,** 1279–1290
16. Nguyen, B. P., Gil, S. G., and Carter, W. G. (2000) *J. Biol. Chem.* **275,** 31896–31907
17. Talts, J. F., Sasaki, T., Miosge, N., Goehring, W., Mann, K., Mayne, R., and Timpl, R. (2000) *J. Biol. Chem.* **275,** 35192–35199
18. Lampe, P. D., Nguyen, B. P., Gil, S., Usui, M., Olerud, J., Takada, Y., and Carter, W. G. (1998) *J. Cell Biol.* **143,** 1735–1747
19. Goldfinger, L. E., Stack, M. S., and Jones, J. C. (1998) *J. Cell Biol.* **141,** 255–265
20. Nguyen, B. P., Ryan, M. C., Gil, S. G., and Carter, W. G. (2000) *Curr. Opin. Cell Biol.* **12,** 554–562
21. Pilcher, B. K., Dumin, J. A., Sudbeck, B. D., Krane, S. M., Welgus, H. G., and Parks, W. C. (1997) *J. Cell Biol.* **137,** 1445–1457
22. Dumin, J. A., Dickeson, S. K., Stricker, T. P., Bhattacharyya-Pakrasi, M., Roby, J. D., Santoro, S. A., Parks, W. C. (2001) *J. Biol. Chem.* **276,** 29368–29374
23. Parks, W. C. (1999) *Wound Repair Regen.* **7,** 423–432
24. DuBridge, R. B., Tang, P., Hsia, H. C., Leong, P. M., Miller, J. H., and Calos, M. P. (1987) *Mol. Cell. Biol.* **7,** 379–387
25. Maruyama, M., Sudo, T., Kasuya, Y., Shiga, T., Hu, B., and Osada, H. (2000) *Brain Res.* **887,** 350–358
26. Nomizu, M., Kuratomi, Y., Malinda, K. M., Song, S. Y., Miyoshi, K., Otaka, A., Powell, S. K., Hoffman, M. P., Kleinman, H. K., and Yamada, Y. (1998) *J. Biol. Chem.* **273,** 32491–32499
27. Lacalle, R. A., Pulido, D., Vara, J., Zalacain, M., and Jimenez, A. (1989) *Gene* (*Amst.*) **79,** 375–380
28. Rees, S., Coote, J., Stables, J., Goodson, S., Harris, S., and Lee, M. G. (1996) *BioTechniques* **20,** 102–108
29. Guex, N., Schwede, T., and Peitsch, M. C. (2000) *Current Protocols in Protein Science* (Coligan, J. E., Dunn, B. M., Ploegh, H. L., Speicher, D. W., and Wingfield, P. T., eds.) Unit 2.8, pp. 1–17, John Wiley & Sons, New York
30. Tisi, D., Talts, J. F., Timpl, R., and Hohenester, E. (2000) *EMBO J.* **19,** 1432–1440
31. Ridley, S. H., Sarsfield, S. J., Lee, J. C., Bigg, H. F., Cawston, T. E., Taylor, D. J., DeWitt, D. L., and Saklatvala, J. (1997) *J. Immunol.* **158,** 3165–3173
32. Brauchle, M., Gluck, D., Di, P. F., Han, J., and Gram, H. (2000) *Exp. Cell Res.* **258,** 135–144
33. Lambert, C. A., Lapiere, C. M., and Ånusgens, B. V. (1998) *J. Biol. Chem.* **273,** 23143–23149
34. Yamamoto, T., Eckes, B., Mauch, C., Hartmann, K., and Krieg, T. (2000) *J. Immunol.* **164,** 6174–6179
35. Wan, Y., Belt, A., Wang, Z., Voorhees, J., and Fisher, G. (2001) *Int. J. Mol. Med.* **7,** 329–334
36. Simons, M., and Horowitz, A. (2001) *Cell Signal.* **13,** 855–862
37. Woods, A., and Couchman, J. R. (2001) *Curr. Opin. Cell Biol.* **13,** 578–583
38. Kheradmand, F., Werner, E., Tremble, P., Symons, M., and Werb, Z. (1998) *Science* **280,** 898–902
39. Thodeti, C. K., Albrechtsen, R., Grauslund, M., Asmar, M., Larsson, C., Takada, Y., Mercurio, A. M., Couchman, J. R., and Wewer, U. M. (2003) *J. Biol. Chem.* **278,** 9576–9584